International Conference on Space Optics—ICSO 2006

Noordwijk, Netherlands

27–30 June 2006

Edited by Errico Armandillo, Josiane Costeraste, and Nikos Karafolas

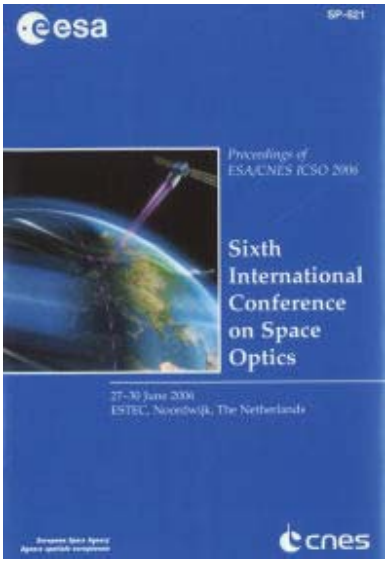

An interferometer for high-resolution optical surveillance from GEO - internal metrology breadboard

L. Bonino, F. Bresciani, G. Piasini, M. Pisani, et al.

International Conference on Space Optics — ICSO 2006, edited by Errico Armandillo, Josiane Costeraste, Nikos Karafolas, Proc. of SPIE Vol. 10567, 1056734 · © 2006 ESA and CNES
CCC code: 0277-786X/17/$18 · doi: 10.1117/12.2308168

AN INTERFEROMETER FOR HIGH-RESOLUTION OPTICAL SURVEILLANCE FROM GEO - INTERNAL METROLOGY BREADBOARD

L.Bonino[(1)] F.Bresciani[(1)], G.Piasini[(1)], M.Pisani[(2)], A. Cabral[(3)], J. Rebordão[(3)], F.Musso [(4)]

[(1)] *AAS-I: Alcatel Alenia Space – Italia, strada Antica di Collegno 253, Torino (Italy); luciana.bonino@aleniaspazio.it*
[(2)] *IMGC: Istituto di Metrologia "G. Colonnetti", now INRiM: Istituto Nazionale di Ricerca Metrologica (Italy); m.pisani@inrim.it*
[(3)] *INETI - Instituto Nacional de Engenharia, Tecnologia e Inovação (Portugal); Jose.Rebordao@ineti.pt; Alexandre.Cabral@ineti.pt*
[(4)] *Politecnico of Torino (Italy) fabio.musso@polito.it*

ABSTRACT

This paper describes the internal metrology breadboard development activities performed in the frame of the EUCLID CEPA 9 RTP 9.9 "High Resolution Optical Satellite Sensor" project of the WEAO Research Cell by AAS-I and INETI. The Michelson Interferometer Testbed demonstrates the possibility of achieving a co-phasing condition between two arms of the optical interferometer starting from a large initial white light Optical Path Difference (OPD) unbalance and of maintaining the fringe pattern stabilized in presence of disturbances.

1. INTRODUCTION

The role of the external and internal absolute metrology is to support the achievement of the Michelson interferometer co-phasing, consisting in the equalization of the optical path lengths of the various arms within a fraction of the coherence length, so that a good visibility fringe pattern is formed at the focal plane of the instrument. The role of the relative metrology is to measure the incremental OPD between the various arms, starting from a given zero optical path difference origin set once the co-phasing condition has been achieved. The control system is capable of controlling the OPD variation within 10 nm once the interferometer co-phasing condition has been achieved.

This interferometer prototype includes a system for injecting OPD disturbances, a delay line for the control of the OPD, breadboards of the absolute metrology (Portuguese part) and of the relative metrology (Italian part) and a control system adapted to this demonstrator.

The laboratory demonstrator of the co-phasing system is capable of reproducing the same basic function of the one defined for the GEO instrument. In particular, it is possible to verify the following functions:

- Measurement of the OPL/OPD between two arms of a Michelson-like interferometer;
- Equalisation of the OPLs within a fraction of the coherence length, so that a good visibility fringe pattern is formed on the focal plane of the instrument;
- Control of the OPD variations within a fraction of the observation wavelength for a significant time duration and under OPD disturbances resembling (and in any case not smaller) those expected on orbit.

2. THE BREADBOARD

The Internal Metrology Sensor Demonstrator is composed of (Fig. 1):

- White light interferometer – the co-phasing condition is verified with the analysis of the white light fringes.
- Absolute metrology – measures the OPD to be compensated by the delay line.
- Relative metrology – after co-phasing is reached, maintains that condition by compensating the induced disturbances.

The detailed optical scheme is shown in figure 2.
The beam collimator (1) generates a parallel white light beam (like that arriving on the GEO instrument from a distant light source) from a point-like source generated by on optical fiber. The aperture mask (2), placed in front of the collimator produces in output two 18 mm diameter, parallel light beams separated by an inter-axis distance of 50 mm. The apertures of the mask act as the light collecting apertures of the two-arms optical interferometer prototype implemented in the breadboard.
The OPD disturbance injection device (3) is used for the introduction of artificial perturbations between the interferometer arms (simulating the ones present in the

Proc. '6th Internat. Conf. on Space Optics', ESTEC, Noordwijk, The Netherlands, 27-30 June 2006 (ESA SP-621, June 2006)

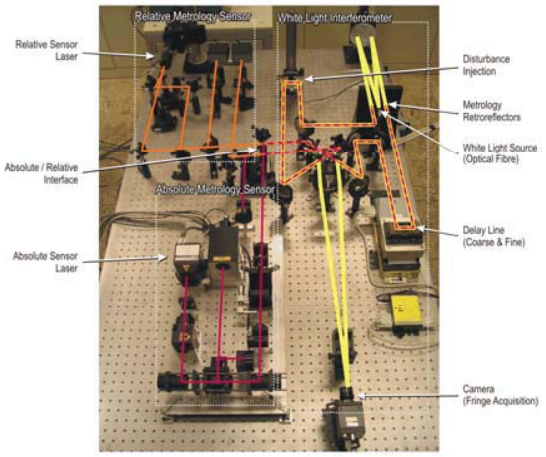

Fig. 1. – The Internal Sensor Demonstrator: how the light travels in all the interferometers.

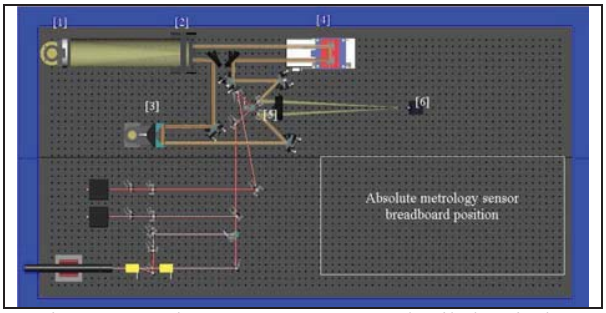

Fig. 2: Internal Sensor Demonstrator detailed optical scheme

real GEO instrument). A coarse / fine delay line (4) is used for the equalisation and control of the OPD between the two arms of the optical interferometer.
A beam combiner (5), focuses on the same point of the focal plane (6) the light beams coming from the two apertures of the optical interferometer thus allowing the formation of the white light interference fringes.
An optical interface allows the injection/extraction of the laser metrology beams in/from the interferometer arms. This interface is constituted by two dichroic mirrors (reflecting the white light and transmitting the metrology laser wavelength) collocated in front of the beam combiner (5). To fold back on themselves the metrology laser beams after they have travelled the same path of the white light beams, two retro-reflectors are foreseen. These retro-reflectors are integrated in the mask apertures and are made by two small Corner Cube Retroreflectors.
In Fig.3 the picture of the complete laboratory setup is shown.

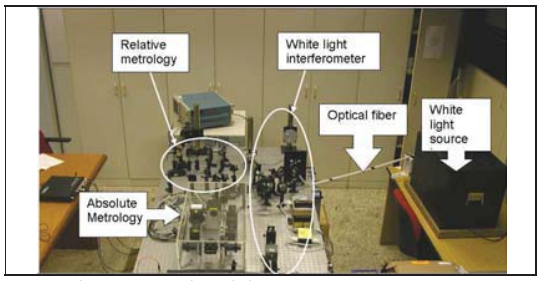

Fig.3: complete laboratory set-up

The Coarse Delay Line (CDL) is capable of an OPD variation of -46 mm to +17 mm from co-phasing.
The CDL position corresponding to the co-phasing condition was measured with the help of the symmetry of the fringe visibility variation with OPD. By scanning around the maximum visibility region, the co-phasing position in the CDL was determined with an error inferior to 1 µm. Fig. 4 shows an example of the type of fringe patterns observed during that process.

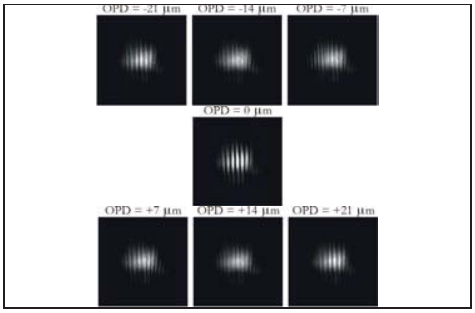

Fig. 4. - White light fringe patterns observed during the determination of the CDL position that corresponds to the co-phasing condition.

3. FSI – FREQUENCY SWEEP INTERFEROMETRY

Frequency Sweeping Interferometry (FSI) was selected to be the absolute distance metrology technique of the EUCLID – RTP 9.9 Internal Sensors breadboard Demonstrator (ISD). The sensor was assembled in the ISD breadboard, to be tested with the relative sensor and the white light interferometer used to demonstrate the co-phasing capabilities of this metrology.

FSI is an interferometric technique capable of measuring the absolute value of the OPD between two arms of a Michelson interferometer (Fig. 5). In this technique, a synthetic wavelength Λ is generated, much longer that the optical wavelength, that increases with decreasing frequency sweep range:

$$\Lambda = \frac{c}{\Delta\nu} \qquad (1)$$

where c is the speed of light and $\Delta\nu$ is the frequency sweep range. In FSI, while the frequency sweeps, detection electronics counts maxima and should be able to determine the fractional part of the fringe at the beginning and at the end of the measurement without ambiguity. In parallel, a Fabry-Perot interferometer (FP) counts resonances in order to measure the frequency sweep range. The measured length (in vacuum) is given by:

$$L = N \cdot \frac{\Lambda}{2}, \quad N = No + \frac{\varphi}{2\pi} \qquad (2)$$

where N is the number of fringes equal to the integer part (N_0) plus the remainder phase φ.

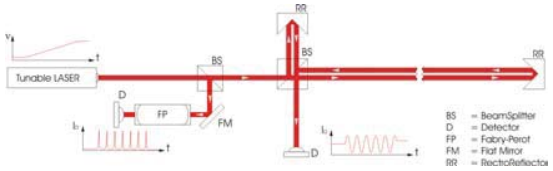

Fig. 5. - FSI optical setup.

In FSI, the range is limited by the largest sweep range available and the capacity of the detection electronics to count integer fringes: the fringes must be post processed, the detection electronics must keep all data, resulting in a limit to the range. Resolution is related to phase measurement uncertainty at the synthetic wavelength and sweep range uncertainty. As range increases, resolution decreases. For small lengths, resolution is driven by phase measurement uncertainty; for larger lengths, resolution is limited by sweep range uncertainty. Fig. 6 shows a picture of the FSI Breadboard for the ISD.

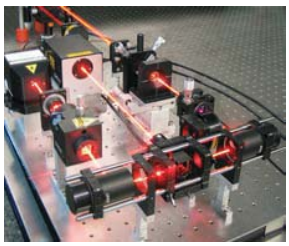

Fig. 6 – FSI Breadboard for the ISD.

3.1 FSI Sensor Tests

The tests performed with the absolute metrology sensors had the following sequence:

1. Evaluation of the vibration noise influence in the FSI sensor performances (noise is determined using the FSI laser in relative mode).
2. Determination of Absolute sensor performances for different OPD values (coarse delay line is moved, covering the complete range, and, at each distance, 500 measurements were performed).
3. Calibration of Fabry-Perot interferometer (FP) Free Spectral Range (FSR)
4. Determination of absolute interferometer OPD offset.
5. Verification of OPD reduction efficiency by the Absolute sensor.

The mechanical vibration noise sensed during the FSI sweep is increased by the amplification factor $\Pi/\lambda 0 \approx 3\,950$. Unfortunately the level of noise in the ISD was considerably large (Fig. 7). Considering the value of the amplification factor, these levels of noise would introduce a 2σ error in the FSI measurement of 89 µm. This would obviously destroy any change of success in the ISD test.

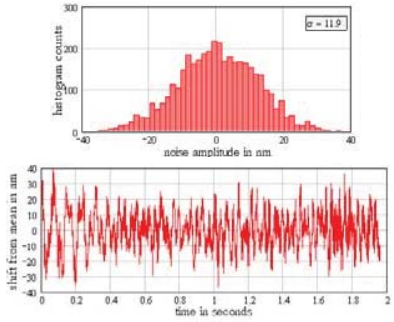

Fig. 7 – Vibration noise in the ISD (with corresponding histograms).

Nevertheless, as seen in Fig. 7, the level of noise is not constant but its mean is always zero and has a normal distribution. Thus, if instead of a single measurement we use a moving average filter, the influence of the noise in the "real time" OPD measurement is reduced.

Two sets of measurements were performed. The first one comprised measurements at the margins of the CDL travel range. With this data, using the CDL accuracy (< 1 µm), the FP FSR was calibrated. Fig. 8 shows an example of a measurement at 11 mm.

When the white light interferometer is co-phased (OPD=0), the OPD in the metrology interferometer is not necessarily null. The distance from the dichroic mirrors (that separates the white light from the metrology laser beams) and the common beam splitter and also the distance from the white light source and the retroreflectors might not be the same for each arm.

Thus, an offset might exist in the metrology interferometer. With a second set of measurements the offset value was determined.

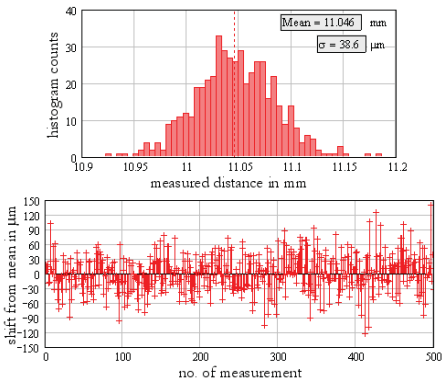

Fig. 8 - Test results obtained in the ISD at 11 mm.

The OPD reduction efficiency of the absolute sensor was tested in a four steps process:

1. move randomly the CDL away from co-phasing;
2. measure the distance from co-phasing with the FSI absolute sensor;
3. move the CDL back to co-phasing, according to the absolute sensor measurement;
4. determine the error from co-phasing.

To overcome the problem of vibration noise, a moving average filter with 25 samples was applied to the measurements.

Fig. 9 shows the results obtained in this test. Errors in the determination of the distance from co-phasing were smaller than 5 µm and, in terms of relative error, smaller than 0.06%.

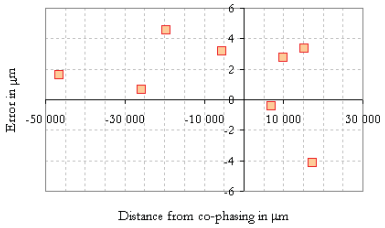

Fig. 9. – Error for real time 25 samples moving average FSI absolute measurements.

3.2 Internal Absolute Metrology Conclusions

For distances (½OPD) up to 46 mm, the measurement error was always less than 5 µm. It must be noted that these results were obtained with considerable vibration noise (during periods of 40 ms noise amplitudes could be as large as 40 nm, with a normal distribution with σ=12 nm).

Previous tests in INETI, with a low level of vibration noise (σ=0.3 nm), made clear the possibility to reach a maximum error smaller than 10 µm. If, for the one hand, the levels of noise in the ISD could jeopardise the absolute sensor test, for the other hand, it allowed the confirmation that, even in a situation where vibration noise cannot be dumped, good results are possible with the use of a moving average filter.

The performances of this sensor can be further improved with more efficient data processing to increase fringe resolution.

The only critical issue remaining is the influence of the noise in the absolute measurements. This influence can be reduced by decreasing the sweep duration and/or the amplification factor (by increasing the laser central wavelength). Optimising these two features, it will be possible to reduce this influence by an order of magnitude, thus enabling FSI to cope with equivalently higher levels of noise. Nevertheless, while the FSI sensor is measuring, the relative metrology can reduce the noise to a level that would not affect that measurement.

The final GEO Instrument will be larger that the GEO Demonstrator by a factor of 5 (from 8m to 40m). The sensor ranges should also increase by the same factor. For the absolute metrology, as the FSI measurement is not ambiguous, this 5× increase will not require any change in sensor specifications.

The laser used in this test was developed by NewFocus and, as a result of their partnership with JPL to develop a laser for cesium atomic clocks in space, it is already space qualified and actually operating in space. The optical and mechanical components are easily adapted to be space qualified. In what concerns the FP, main component in the frequency sweep measuring sub-system, the space qualification should be the main focus of a next phase.

4. RELATIVE LASER METROLOGY

For measuring the variations of the length between the two arms of an optical interferometer, the choice naturally falls on a laser interferometer of Michelson type implemented in heterodyne version; the concept is shown in Fig. 10. Two different light sources having different frequencies υ_1, υ_2 are sent in the two arms. After the forth and back trip, the beams are again recombined on the detector and now the signal is a beat note having frequency $\nu = |\nu_1 - \nu_2|$ and a phase which varies with the optical path difference.

The corresponding laboratory setup is shown in Fig.11 and 12.

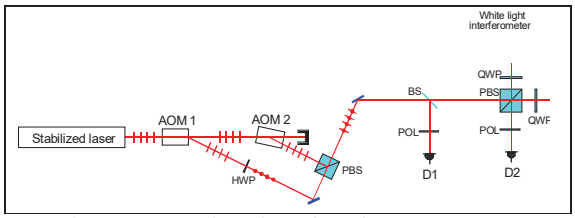

Fig. 10: Heterodyne laser interferometer concept (relative metrology)

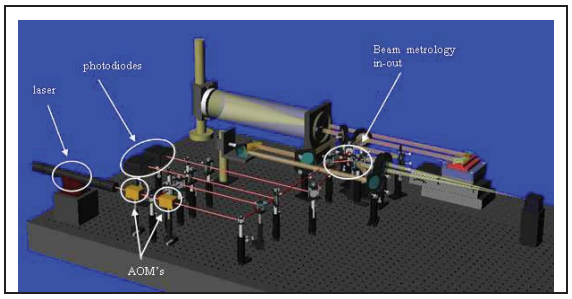

Fig. 11: relative metrology optical bench setup

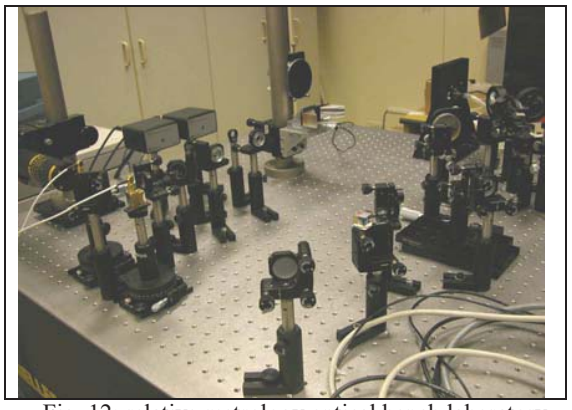

Fig. 12: relative metrology optical bench laboratory implementation

4.1 Relative Metrology Sensor Tests

As a first step we have achieved the interferometer co-phasing condition by commanding the optical delay line in open loop, on the basis of the measurements provided by the absolute metrology and to the feedback provided to the operator by the image of the fringe pattern on the focal plane. Once the quality of the fringes is considered adequate, the control system operates in closed loop with the relative laser metrology to keep the fringe pattern frozen (i.e. the OPD frozen) over all the observation period.

The setup is subject to environmental and artificially injected disturbances; the injected disturbance spectrum is an envelope of several possible realisations of disturbance profiles that may affect the instrument on the spacecraft, originated e.g. by opening / closing of thruster valves, reaction wheels, etc. It has been developed as a reasonable hypothesis of work for a study phase, but a more accurate study involving spacecraft mechanical simulations would be necessary to find the expected disturbances spectrum for a GEO interferometer, as it strongly depends on the spacecraft structure configuration and physical properties.

The injected optical path difference disturbances power spectral density is shown in Fig. 13.

Note that the laboratory environment noise increases the injected disturbance: this effect is shown in Fig.14, where the blue curve is the injected disturbance, the green curve is the environmental disturbance, the azur blue curve is the total disturbance due to the sum of the two effects.

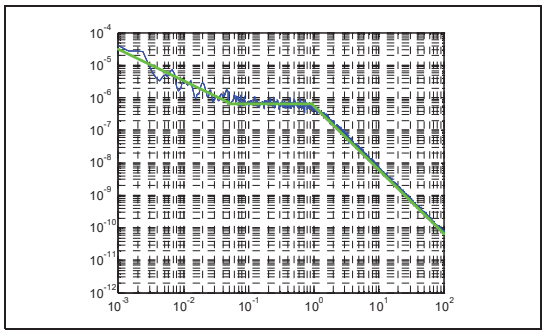

Fig.13: Expected asymptotic OPD disturbance PSD (green) and the generated one (blue)

The test performed show that both the tracking mode and the OPD control are possible and quite robust. The goal of the test - i.e. to validate the concept of the co-phasing control in order to keep it in a 10 nm at 1σ range - is fully achieved, as it is possible to see in Fig.15. All the expected results are compliant with the experimental results, thus validating the control system design procedure and its performance.

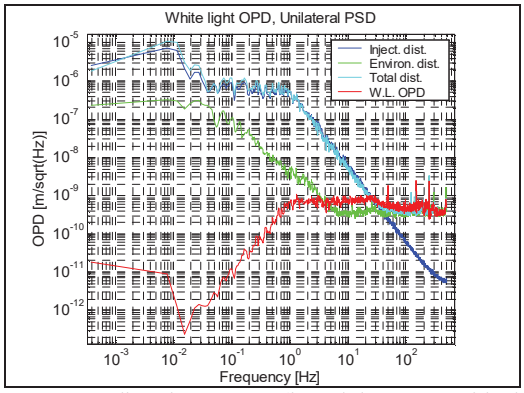

Fig.14: OPD disturbance PSD (in red the OPD residual variation)

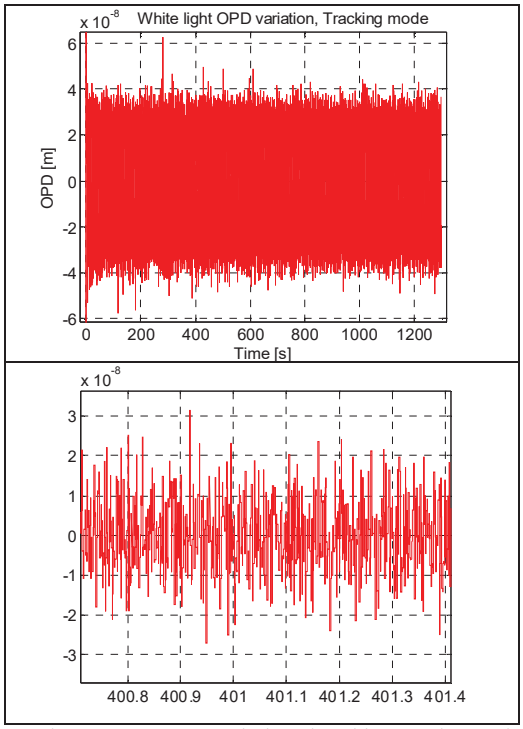

Fig. 15: up, OPD variation time history; down, detail

Time duration of tracking mode is not limited by the control system performance (test reported are about twenty minutes long, but other test of forty minute long and more have been performed with the same results), but only by the stroke of the delay line fast actuator (the PiezoTranslator, PZT). If the OPD disturbance exceed twice of control PZT stroke (twice because there are two reflection in the delay line), the OPD controller is of course not capable of compensating them completely.

To better show the disturbance compensation action of control system, a in-tracking mode test with continuous disturbance injection and an alternate on/off condition of closed loop OPD control has been made. Stopping the closed loop disturbance compensation, the OPD follow the injected disturbance, starting the closed loop disturbance compensation, if the disturbance in non closed loop condition not bring the OPD far to the co-phased condition, the OPD came back to co-phased condition OPD and control system keep it into a required range. In Fig.16 it is shown the measured OPD time history with starting/stopping the closed loop disturbance compensation. This performance exceeded expectations showing the control robustness.

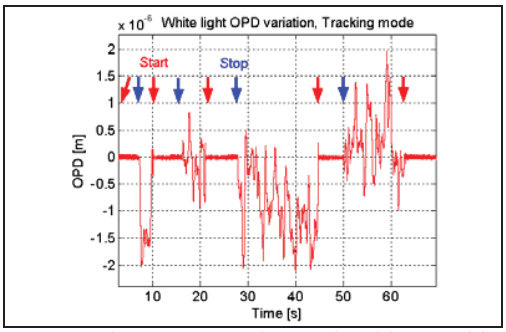

Fig.16: measured OPD time history with starting/stopping the closed loop disturbance compensation

4.2 Internal Relative Metrology Conclusions

The technological maturity of this kind of cophasing systems is quite good for what concerns the on-ground applications: the metrology interferometer configuration that has been used is the classical heterodyne one, well known and extensively used both for scientific and industrial applications from more than 30 years; the delay line is based on a two-stage translator (motorised linear translator and PZT translator) using standard technology.

The results derived from the breadboard tests show the technical feasibility of the cophasing system. In particular, it has to be considered that the breadboard has been built using only off-the-shelf devices, except some particular optical elements that are custom, produced following geometrical specifications, but that didn't require any particular technological effort by the manufacturer. Also from the point of view of control and electronics there is no critical aspect, all the algorithms, techniques and devices involved are well known and extensively used.
So the co-phasing system based on internal (relative) sensors can be considered mature both from feasibility and technology point of view, for what concern a breadboard-level implementation.